SAE Technical Paper 2022-01-0466

Investigation of a Second Exhaust Valve Lift to Improve Combustion in a Methane - Diesel Dual-Fuel Engine

Mueller F.[1], Guenthner M.[1], Weigel A.[1], Thees M.[1]
[1]Universitiy of Kaiserslautern

Abstract

In recent years, the utilization of dual-fuel combustion has gained popularity in order to improve engine efficiency and emissions. With its high knock resistance, methane allows operation in high compression diesel engines with lower risk of knocking. With the use of diesel fuel as an ignition source, it is possible to exploit the advantages of lean combustion without facing problems to provide the high amount of ignition energy necessary to burn methane under such operating conditions. Another advantage is the variety of sources from which the primary fuel can be obtained. In addition to fossil sources, methane can also be produced from biomass or electrical energy.

As the rate of substitution of diesel by methane increases, the trade-off between nitrogen oxide and soot is mitigated. However, emissions of carbon monoxide and unburned methane increase. Since carbon monoxide is toxic and methane has 25 times the global warming potential of carbon dioxide, these emission components pose a problem. Because of the stability of the molecule, methane catalysts require an exhaust gas temperature of over 500 °C in order to work effectively.

In this work, the effect of conventional cooled external exhaust gas recirculation (EGR) and additional hot internal EGR are investigated for different substitution rates in a nonroad tractor engine converted to dual-fuel operation. The internal EGR rate is controlled by a variable second exhaust valve lift during the intake stroke – an approach which promises to benefit dual-fuel engines by increasing the in-cylinder gas temperature, thus favoring more complete combustion. A simulation model of the engine is used to determine the internal EGR rates and in-cylinder temperatures based on the experimental data. When internal EGR is used in combination with external EGR, the resulting emissions show additional reductions in nitrogen oxide (up to -51 %), carbon monoxide (up to -18 %) and methane (up to -28 %) with increasing internal EGR, while still maintaining low soot levels due to the substitution of diesel fuel for methane.

1. Introduction

In the development of internal combustion engines, efficiency and pollutant emissions are two of the most important aspects. Increasing efficiency conserves resources and reduces emissions of the greenhouse gas carbon dioxide. Lowering pollutant emissions such as soot and nitrogen oxides helps to reduce the complexity of the exhaust gas aftertreatment system while still complying with the relevant exhaust gas regulations. These two issues also play a major role when using renewable fuels. While the climate impact is mitigated by the use of such fuels, their limited availability still makes it necessary to achieve high combustion efficiency. One way of reaching both of these goals is the utilization of a dual-fuel combustion, which is investigated for a nonroad tractor engine in this paper.

1.1 Dual-Fuel Combustion

In a dual-fuel engine, two fuels are used simultaneously. This involves a main fuel, which provides most of the chemical energy for combustion, and an ignition fuel, which initiates the combustion of the mixture.

For diesel dual-fuel engines, this makes it possible to ignite lean mixtures beyond the limits of spark ignition. Even low-reactivity fuels such as methane can be burned with high air-fuel ratios in this way [1], [2].

Another advantage is the possibility to run the engine on 100% diesel or any other reduced substitution rate as required. Diesel engines are also relatively easy to convert to dual-fuel operation, and their compression ratio makes it possible to achieve high efficiency levels.

However, modern diesel engines are not designed to operate with a homogeneous air-fuel mixture, which is why increased emissions of unburned hydrocarbons are observed when running such an engine in dual-fuel mode. The increase in carbon monoxide emissions may also present a problem [1]. This can be addressed by changing the combustion process or by making modifications to the engine hardware [3].

The main fuel can be supplied in a number of ways. It can be injected or mixed centrally into the intake system, or injected individually for each cylinder using port injection. Another possibility is direct injection into each cylinder [4]. For the combustion process, this means a transition from a diesel diffusion flame to a laminar flame like in a spark ignited gas engine. The process employed for the current study might be characterized as Homogeneous Charge Induced Ignition (HCII). Yu et. al. [5] showed the potential of HCII for high thermal efficiency at low nitrogen oxide and soot emissions. When utilizing high EGR ratios, so-called low temperature combustion (LTC) revealed to be possible, decreasing nitrogen oxides and soot even further. Normally, LTC is achieved by the compression ignition of the low reactivity fuel with or without a trigger through a high reactivity fuel (such as diesel). This trigger raises the mixture reactivity and initiates auto-ignition. There are several approaches to LTC through this method, such as

Homogeneous Charge Compression Ignition (HCCI), Premixed Charge Compression Ignition (PCCI) and Reactivity Controlled Compression Ignition (RCCI). In the case of dual-fuel HCCI, both fuels can be premixed before the intake stroke by port injection. Even though a variation of the ratio between the primary and secondary fuel provides some sort of control of combustion phasing (as shown by Stanglmaier et al. in [6]), this issue is still considered as one of the main obstacles for the practical realization of this process. Kokjohn et al. [7] investigated an approach where the high reactivity fuel was added by a single early direct injection, giving the mixture enough time to homogenize. They observed very low nitrogen oxide and soot emissions, but the process required EGR rates of nearly 60 % to control combustion phasing in operation with diesel fuel. In the same work, a PCCI approach is investigated, which was realized by injecting the secondary fuel later during the compression stroke using two injection events. This improved the controllability of combustion, while still maintaining low soot and nitrogen oxide emissions. For RCCI combustion, Reitz et al. [8] used the different reactivity of the two fuels employed for combustion control. As a result, thermal efficiency increased even further, with emissions of nitrogen oxides and soot remaining at very low levels. RCCI is considered a promising approach to LTC, with several studies focusing on this combustion process [9], [10], [11].

1.2 Methane as a Fuel

Methane can be obtained from various sources. In addition to occurring as a major component of natural gas, methane can be produced from biological sources as well as synthetically.

For the production from biomass (biomass to gas, BtG), for example, waste from many sources can be used (e.g. landfills, livestock, sewage treatment plants) [12]. This avoids competition with food production and allows to exploit otherwise unused sources of energy.

Synthetic methane (power to gas, PtG) is obtained using water electrolysis to first produce hydrogen, which is then methanated in a reaction with CO or CO_2. Compared with the direct use of hydrogen, this means an additional process step and thus a reduction in overall efficiency of the process; however, methane is easier to store and can be fed into the existing natural gas network in high quantities [13].

When used as a fuel in an internal combustion engine, the high anti-knock properties of methane are advantageous. This makes it suitable for use in high compression diesel engines and enables high substitution rates in dual-fuel operation. However, methane requires high ignition temperatures of 600 °C, which makes complete combustion of the homogeneous air-fuel mixture difficult [14]. Due to the stability of the methane molecule, special catalysts are needed for exhaust gas aftertreatment, which have light-off temperatures of over 500 °C and thus place special demands on exhaust gas temperature management [15]. Since the global warming potential (GWP) of methane is 25 times that of carbon dioxide, it is essential that the conversion by the catalytic converter be as complete as possible [16].

1.3 Exhaust Gas Recirculation

In order to reduce the emissions of unburned methane in dual-fuel combustion engines, the completeness of the combustion process needs to be improved. This can be achieved by elevating the charge temperature through exhaust gas recirculation. The working principle of exhaust gas recirculation (EGR) is to introduce exhaust gas into the fresh cylinder charge. Exhaust gas exhibits an increased specific heat capacity compared to air because of the increased proportion of triatomic molecules (CO_2, H_2O). EGR slows down combustion and displaces fresh air, thus reducing the oxygen content of the mixture [17], [18]. As a result, peak combustion temperatures drop, which in the case of diesel engines leads to a reduction in nitrogen oxide emissions and an increase in soot. The charge temperature, however, is increased by the higher temperature of the exhaust gas compared to the fresh air, which in turn is advantageous for dual-fuel operation.

There are several ways to add recycled exhaust gases to the combustion. As a very common example, Figure 1 shows an external high-pressure EGR loop which is cooled by the engine coolant through a gas-to-water heat exchanger. On the right-hand side of the drawing, the valve lift curves are shown schematically.

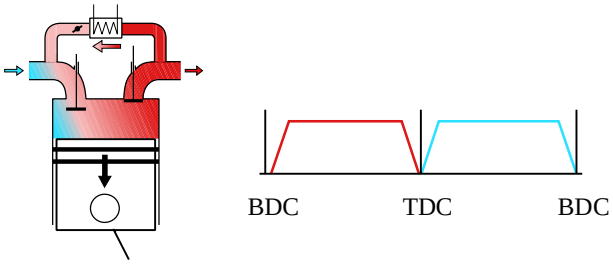

Figure 1. External high-pressure EGR (cooled)

The amount of recirculated exhaust gas is controlled by a valve in the EGR loop. As the pressure difference between exhaust and intake may be a limiting factor when the EGR valve is already fully opened, an additional throttle in the exhaust system may be used in order to increase back pressure and thus allow higher EGR ratios.

On the test bench, the EGR rate (x_{EGR}) is determined by analyzing the CO_2 content in the intake system ($c_{CO_2,Intake}$) and the exhaust system ($c_{CO_2,Exhaust}$). It is calculated according to the following formula:

$$x_{EGR} = \frac{c_{CO_2,Intake} - c_{CO_2,Ambient}}{c_{CO_2,Exhaust} - c_{CO_2,Ambient}} * 100\,\% \quad (1)$$

For the application to increase the charge temperature, a higher temperature of the EGR is desirable. Because of thermal limitations of the components in the intake system, such an increase is not possible with the external system. To solve this issue, it is possible to use so-called “internal EGR” by choosing an appropriate valve opening strategy. A potential realization is shown in Figure 2.

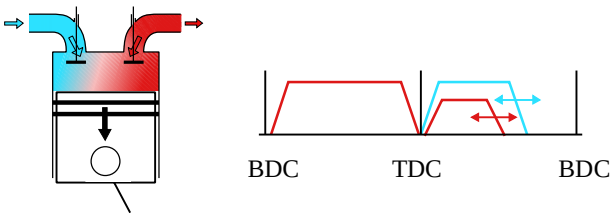

Figure 2. Internal EGR by exhaust gas rebreathing (uncooled)

There are different ways of realizing internal EGR. For the current work, the focus is on so-called “exhaust gas rebreathing”. In gasoline

engines, this can be achieved by simply extending or shifting the exhaust valve opening past TDC and into the intake stroke. On the contrary, similar to Diesel engines, this is not possible for the engine used in the experiments here due to its high compression ratio, as otherwise a collision between piston and exhaust valve would be the result. Also, the quantity of exhaust gas which can be rebreathed into the cylinder would be limited to a very small amount, and the exhaust stroke would be compromised because of the delayed exhaust valve opening. Therefore, a second exhaust valve lift (in the following referred to as "2nd event") was implemented on the test engine. Here, gas is simultaneously drawn in from the intake system via the two intake valves and from the exhaust manifold by opening one of the exhaust valves during the intake stroke. This is illustrated by the schematic valve lift curves in Figure 2.

The real valve lifts of the engine will be discussed in the following chapter. The amount of EGR is controlled by the lift and duration of the 2nd event. As it is difficult to measure the quantity of internal EGR, it was calculated by a simulation model using the intake, cylinder and exhaust pressure as recorded by the pressure indication system. A combination of external and internal EGR is also possible in order to increase EGR rates even further than with one system alone.

Dev et al. [19]. investigated the impact of external EGR on a natural gas-diesel dual-fuel engine and reported a decrease in hydrocarbon emissions due to the longer combustion duration. Shim et al. [20] showed that especially hot external EGR can reduce hydrocarbon emissions and improve efficiency.

Buitkamp [21] and Thees et al. [22] showed the potential of a second exhaust valve lift for thermal exhaust gas management in a nonroad diesel engine. Gonzalez et al. [23] compared internal EGR to other measures for raising exhaust gas temperatures and reducing emissions, proving its effectiveness in steady-state and transient operation for a Euro 6 passenger car diesel engine. Willand et al. [24] used exhaust gas rebreathing as a measure to control auto-ignition in a gasoline engine for the Volkswagen GCI (gasoline compression ignition) combustion process.

The work presented here builds upon the findings from the external EGR investigations in dual-fuel operation and from the use of internal EGR in diesel operation, and aims at investigating the effects of combined internal and external EGR on dual-fuel combustion.

2. Experimental Setup

All of the tests were conducted on a John Deere 4045 engine which was modified for the study. Table 1 shows the technical data of the base engine.

Table 1. Technical data of the JD4045 engine.

	Value	Unit
Rated Power	130	kW
Rated Speed	2100	rpm
Peak Torque (@ 1600 rpm)	703	Nm
Displacement	4.5	dm^3
Stroke	127	mm
Bore	106.5	mm
Compression Ratio	17.3:1	-
Valves per Cylinder	4	-
Emission Standard	EU Stage IV	-

Although the base engine complies with the former EU Stage IV emission standard, the reference for the tests was EU Stage V, since this is the current standard. Table 2 shows the according limits for the individual exhaust gas components.

Table 2. EU Stage V emission limits [25].

	Value	Unit
CO	5.0	g/kWh
HC	0.19	g/kWh
NO_x	0.4	g/kWh
PM	0.015	g/kWh
PN	1×10^{12}	#/kWh

In order to use different 2nd event valve lifts, the engine was converted from its overhead valve (OHV) design with one lateral camshaft to a mechanically fully variable double overhead camshaft (DOHC) layout. This required a strongly modified cylinder head design including the new valvetrain components (Figure 3). The design, manufacturing and test of this new cylinder head and valvetrain concept has already been carried out in the context of previous projects at the institute. It is built as a two-piece design. The upper part carries the valvetrain mechanics, whereas the lower part serves more as a traditional cylinder head, housing the valves, water jacket and ports. More details of the engine and the cylinder head concept can be found in [21], [22] and [26].

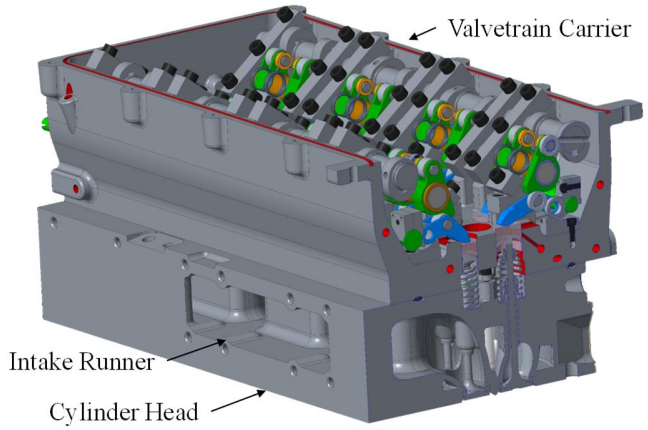

Figure 3. Modified cylinder head with dual fully variable valvetrain (view from intake side)

The new valvetrain allows the realization of different concepts for the variation of the valve lift on both the intake and the exhaust side. The layout used here includes fully variable intake valve lift and a variable second event on the exhaust side. On the inlet side, the valve lift is variable between 0 and 7.3 mm. The 2nd event lift is only installed on one of two exhaust valves per cylinder and can be adjusted continuously between 0 and 1.9 mm. However, this adjustment also influences the main lift of the corresponding exhaust valve, which is reduced from 8.8 mm at full 2nd event down to 5 mm for no 2nd event. For the second exhaust valve of each cylinder, the lift is fixed at 8.4 mm and cannot be varied. Figure 4 shows this characteristic of the actual valve lift curves as measured by means of a laser vibrometer on the component test bench of the institute.

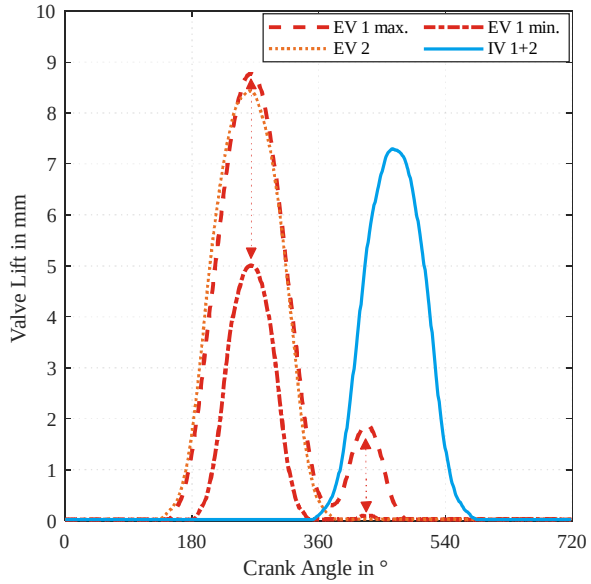

Figure 4. Measured valve lift characteristic

The shown curve of “EV 1 max.” corresponds to 1.9 mm 2nd event case as presented in the results of this study. Its main lift during the exhaust stroke also corresponds to the exhaust valve lift of the original engine. The “EV 1 min.” curve stands for the 0 mm 2nd event case on the following pages.

Another necessary modification of the base engine was the installation of a spacer between cylinder head and EGR mixer. This spacer carries four Bosch CNG injectors and also serves as a mounting base for the methane fuel rail. Due to the design of the intake manifold and its integration into the cylinder head, it was not possible to place the injectors directly in front of the individual intake ports (as obvious from the integrated intake runner visible in Figure 3).

The test engine was connected to a Schenck W400 eddy current dynamometer, and an asynchronous electric motor with an overrunning clutch was used for motoring. All of the cylinders were fitted with Kistler 6056 piezoelectric pressure sensors by the use of Kistler glow plug adapters. On the intake and exhaust side, Kistler 4011 piezoresistive low-pressure transducers were installed. For the detection of the crank angle, a Heidenhain ROD 426 rotary encoder with a resolution of 0.1 °CA was attached to the engine’s crankshaft. The pressure indication for the four cylinders, the intake and the exhaust manifold was carried out by an AVL Indimodul 621 with the corresponding IndiCom software. Omega Engineering PXM 319 pressure transducers coupled to Wachendorff ST3218 analog input modules were used for logging the quasi-static pressure values at several additional positions in the engine via LabVIEW. For airflow measurement, an ABB Sensyflow FMT700-P thermal mass flowmeter was used, while the mass flow of the diesel fuel was determined by an AVL FuelExact Coriolis flow meter, which was also used for conditioning the fuel to a constant temperature of 40 °C. The methane consumption was measured by an Endress+Hauser Cubemass C300 Coriolis mass flow meter. In order to determine the actual valve lifts, the eccentric shafts were fitted with Novotechnik RSC-2841 rotary sensors. A Horiba MEXA-6000FT Fourier transfer infrared spectrometer was used in combination with a TESTA FID 1230 flame ionization detector and a Rosemount OXYNOS 100 paramagnetic photodetector to determine the gaseous exhaust gas components, while an AVL Micro Soot Sensor recorded the particle concentration in the exhaust gas. For determining the EGR rate, a Rosemount Binos 1.1 nondispersive infrared sensor was connected to the intake manifold to measure the CO_2 content of the fresh charge prior to combustion. Turbocharger speeds were measured by eddy current sensors from Micro Epsilon.

Figure 5 shows a schematic of the test bench setup.

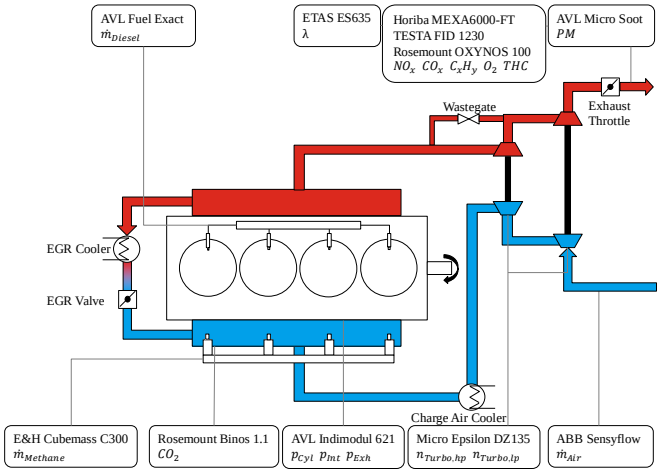

Figure 5. Schematic test bench setup

All of the tests were conducted using the original John Deere ECU. EGR valve and exhaust throttle position, injection timing and pressure as well as the number of injections were set independently from the normal maps in order to keep these parameters constant. Since the torque was set by the eddy current dyno, the ECU could only adjust the fuel quantity of the main injection in order to maintain the demanded engine speed. By injecting methane through the MPI system, the required quantity of the main diesel injection decreases, which is automatically accounted for by the ECU. The injectors of the methane fuel system were controlled by a MoTeC M800 ECU which made it possible to use sequential fuel injection. Therefore, the individual fuel quantities for each cylinder could be controlled in order to account for the differences in air mass distribution between the cylinders.

For the simulative post-processing, a GT-POWER three pressure analysis (TPA) model was used, see Figure 6. Since the inlet and exhaust pressure sensors were installed in proximity to cylinder 4, the corresponding cylinder pressure was used.

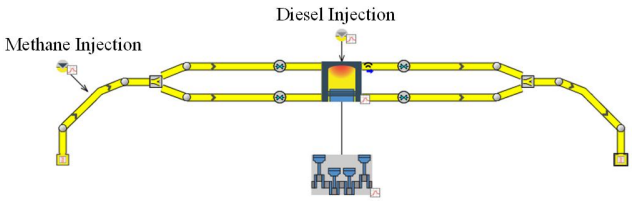

Figure 6. TPA model for cylinder 4

During the design of the cylinder head, extensive 3D CFD simulations have been conducted to determine swirl levels and discharge coefficients of the valves for the TPA model [22]. The model has been validated in the context of a previous project, during which the valvetrain and cylinder head have been developed and tested [21], [22], [26]. In addition, the experimental data of the current investigation has been used to validate the model in dual-fuel operation.

3. Methodology of the Experiments

For the experiments presented in this work, an intermediate load point of 350 Nm was chosen, which equals a BMEP of 9.8 bar. This represents 50 % of the maximum engine torque at 1600 rpm, which represents the engine speed for rated torque and is therefore relevant for the Non-Road Steady Cycle (NRSC) and the World Harmonized Stationary Cycle (WHSC). Furthermore, it is possible to stay within the maximum permissible cylinder pressure limit without the need to retard the combustion at this load point. The effective torque and speed of the engine were kept constant, which means that the IMEPs (and therefore the combined energy input of the two fuels) varied depending on engine efficiency resulting from the different variations (comprising substitution rate, external and internal EGR).

To analyze the effects of methane injection and the introduction of EGR on the gas exchange, the exhaust throttle was always kept wide open and the intake valves remained at their full lift. This means that for every measuring point, the engine was running as lean as possible. Since the engine does not offer any means for controlling the wastegate of the turbochargers, this also leads to a direct effect of the EGR rate on the boost pressure. The charge air was cooled to 25 °C by a conditioned water-to-air intercooler.

Substitution rates were varied from 0 % to 75 % in steps of 25 %. The substitution rate ($x_{Substitution}$) was defined as the ratio between the energy (as a product of fuel mass-flow $\dot{m}$ and lower heating value LHV) provided by the injected methane and the total energy supplied by diesel fuel and methane combined,

$$x_{Substitution} = \frac{\dot{m}_{Methane} * LHV_{Methane}}{\dot{m}_{Methane} * LHV_{Methane} + \dot{m}_{Diesel} * LHV_{Diesel}} * 100\,\% \quad (2)$$

For every substitution rate, the external EGR rate was then varied from 0 % up to 25 % (if possible) with an increment of 5 %. Finally, the 2nd event valve lifts of 0, 0.5, 1.0, 1.5 and 1.9 mm were measured for each combination of substitution rate and external EGR rate.

For every measurement, the center of combustion was kept constant at 8 °CA ATDC, and the diesel rail pressure was set to 170 MPa. The fuel temperatures were 40 °C for diesel fuel and 30 °C for the injected methane.

4. NO_x - Soot Trade-Off in Dual-Fuel Combustion

From conventional diesel combustion, the NO_x - soot trade-off is a well-known phenomenon. By reducing NO_x raw emissions through EGR, soot emissions increase due to the reduction in combustion temperature especially in locally rich areas [27].

Figure 7 shows this behavior for two 2nd event valve lifts using only diesel fuel. For this investigation, the EGR rate was increased in 5 % steps until λ fell below 1.5. The “0 mm 2nd event” curve represents the situation without internal EGR. Here, the soot limit was reached at 27 % external EGR, which is the last point at the top in the diagram. The “1.9 mm 2nd event” curve represents the maximum possible internal EGR. Here, the external EGR rate was limited to 22 %. This is also the point at the top of the corresponding curve in Figure 7.

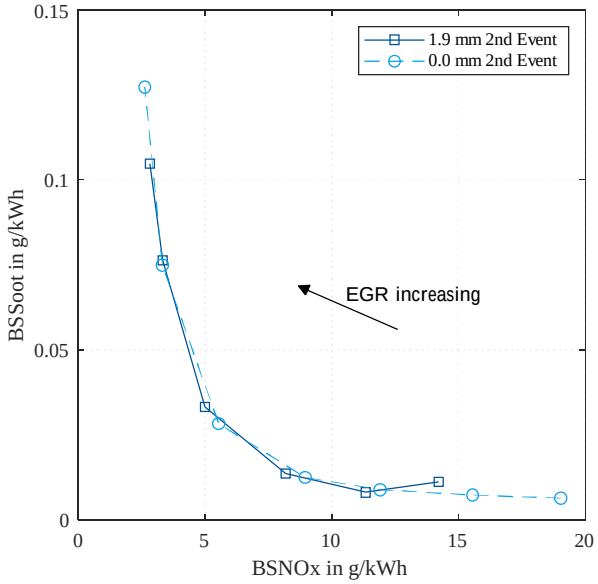

Figure 7. NO_x - soot trade-off for different 2nd event valve lifts (1600 rpm, 350 Nm), measured values

The curve for 1.9 mm 2nd event starts at a lower NO_x level because of the additional internal EGR. However, the courses of both curves coincide almost perfectly.

As soon as diesel fuel is substituted by methane, a mitigation of the NO_x - soot trade-off can be seen. In Figure 8, this is shown for a 2nd event of 0 mm with 5 % steps in EGR rate increase.

Rising substitution rates make it possible to increase the external EGR ratio without the penalty of strongly increasing soot emissions while still reducing nitrogen oxides. Compared to a maximum of 20 % external EGR without methane injection, external EGR rates of over 25 % could be reached.

Even without the aid of EGR, both NO_x and soot emissions dropped with the increase of the methane content. The reduction in soot can be explained by the decrease in diesel fuel mass and the soot-free combustion of methane. The combustion process changes from a solely diffusion-controlled combustion to a predominantly homogeneous lean combustion involving a flame front.

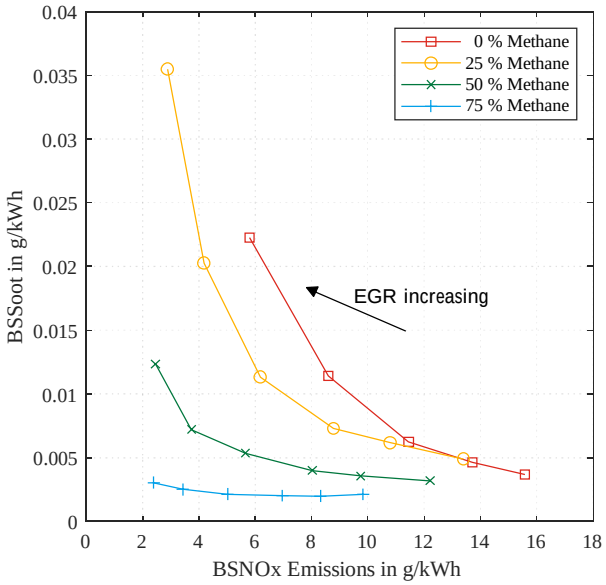

Figure 8. NO_x - soot trade-off for different substitution rates at 0 mm 2nd event (1600 rpm, 350 Nm), measured values

This also leads to a reduced peak temperature during combustion, which can be derived from the TPA calculation as displayed in Figure 9.

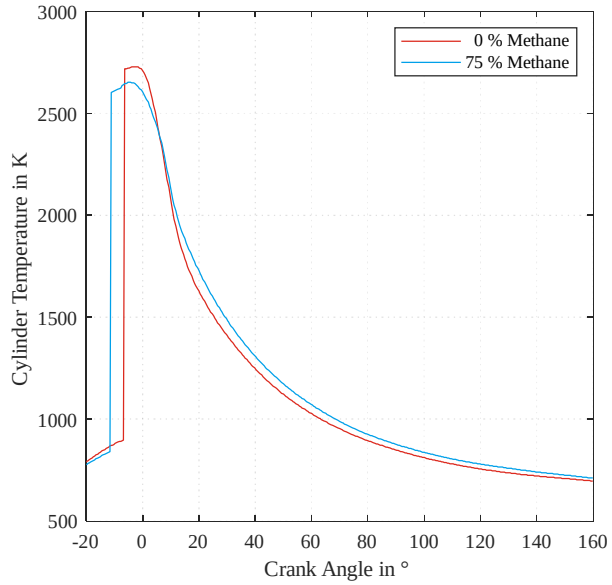

Figure 9. Progression of in-cylinder temperature of the burned zone according to TPA calculation at 0 mm 2nd event (1600 rpm, 350 Nm), calculated values

According to the Zeldovich mechanism, NO_x develops at temperatures above 2200 K in the presence of oxygen [18]. Since the forward and reverse rate constants depend exponentially on temperature [28], the longer period above 2200 K for the 75 % methane case is overcompensated by the higher peak temperatures at 0 % methane. Also, the share of oxygen in the combustion chamber is decreased by introduction of methane into the intake plenum.

Figure 10 shows the corresponding heat release rates for both cases. The center of combustion is the same at 9 °ATDC, but the burn duration increases from 16.2 °CA for 0 % methane (diesel SOI - 8 °CA) to 18.2 °CA for 75 % methane (diesel SOI - 12 °CA). Regarding the burn rate for the 75 % methane case, the curve shows two distinct sections. The first section represents the combustion of the injected diesel fuel, which in turn ignites the methane of the base mixture, thereby initiating the second part of the combustion [19]. This second phase of the combustion process is more rapid, which explains the difference of only 2 °CA in burn duration despite of the difference of 4 °CA in diesel injection timing.

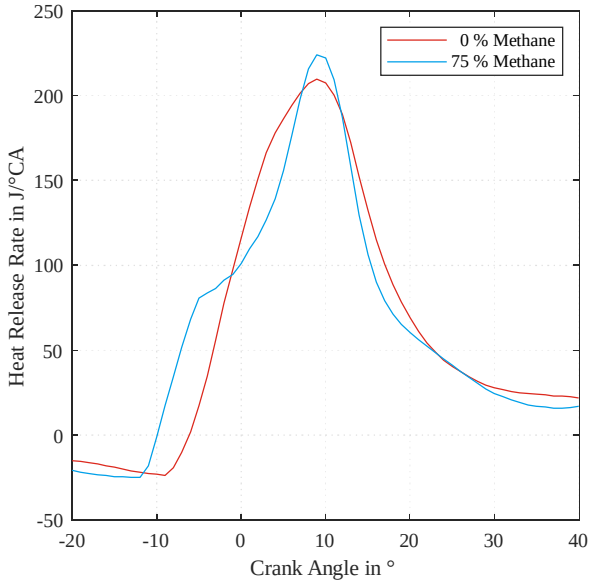

Figure 10. Heat release rates for 0 % and 75 % Methane substitution at 0 mm 2nd event (1600 rpm, 350 Nm), measured values

The peak cylinder pressures shown in Figure 11 are very similar for both cases. The center of combustion was identical at 9 °CA ATDC, but with 75 % methane, the maximum cylinder pressure occurs a few degrees later than in diesel-only operation.

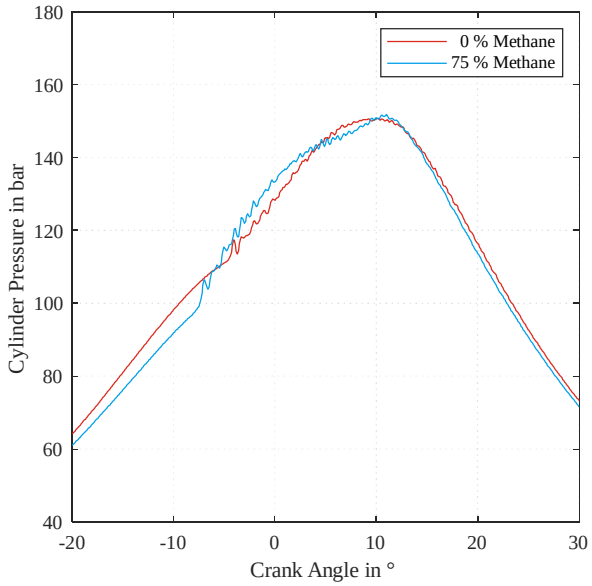

Figure 11. Cylinder pressure curves for 0 % and 75 % Methane substitution at 0 mm 2nd event (1600 rpm, 350 Nm), measured values

5. Carbon Monoxide and Methane Emissions in Dual-Fuel Combustion

Raising the methane content in a dual-fuel combustion process leads to an increase in emissions of both carbon monoxide and unburned methane, as illustrated in Figure 12 and Figure 13.

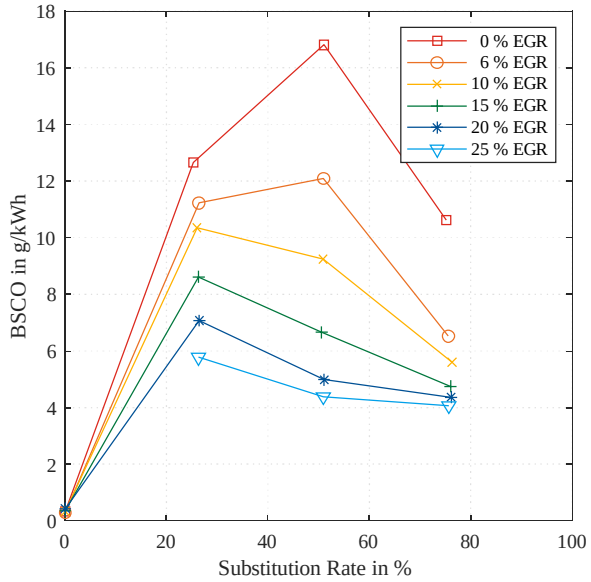

Figure 12. CO emissions depending on substitution rates for different external EGR rates at 0 mm 2nd event (1600 rpm, 350 Nm), measured values

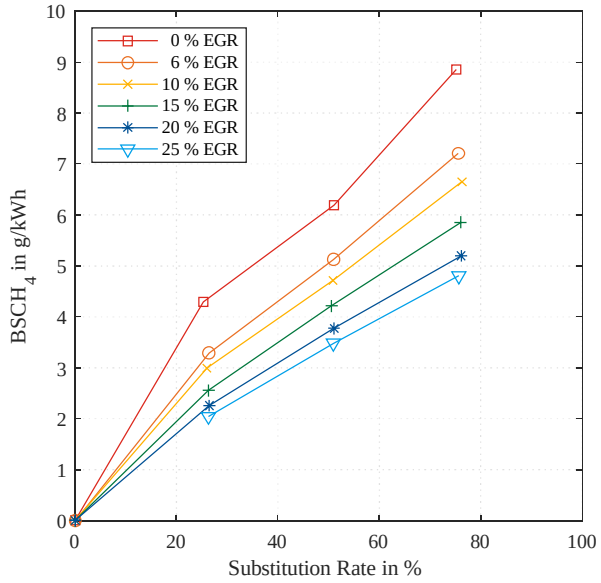

Figure 13. CH_4 emissions depending on substitution rates for different external EGR rates at 0 mm 2nd event (1600 rpm, 350 Nm), measured values

It is also obvious that external EGR is an effective countermeasure against both CO and CH_4 emissions. Figure 12 shows that CO first increases with higher substitution rates and then drops again. The curve for 0 % external EGR shows a CO value of 16.8 g/kWh for a methane content of 50 % and 10.6 g/kWh for 75 % substitution rate. The explanation for this behavior can be derived from Figure 14.

This diagram shows a carbon balance with respect to the carbon input from the two fuels, put into relation to the emission components generated through combustion. The emissions are separated into four categories:

- Fully oxidized, gaseous (CO_2)
- Partly oxidized, gaseous (CO)
- Fully unoxidized, gaseous (CH_4)
- Fully unoxidized, non-gaseous (Soot)

With a rise in substitution rate, the share of the fully oxidized gaseous emission decreases. Since the mass of carbon bound in soot is negligible (especially for higher substitution rates), most of the gap is caused by partly oxidized and fully unoxidized gaseous emissions. The course of the corresponding curves shows that combustion becomes more and more incomplete [29]. This leads to a point where the partly oxidized share drops and the fully unoxidized portion dominates.

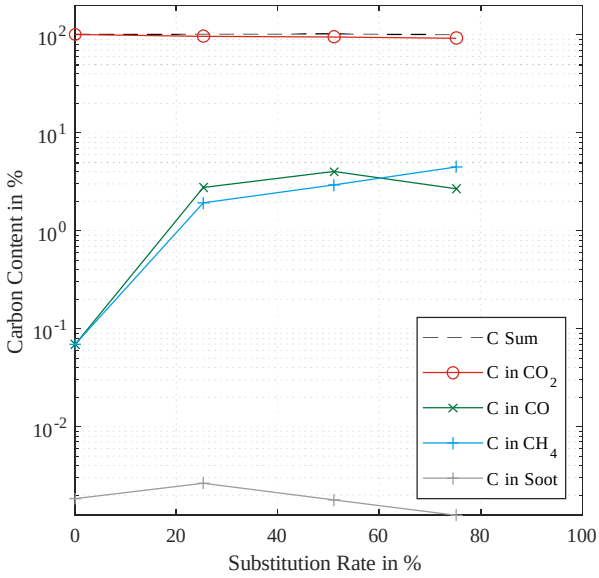

Figure 14. Carbon balance for different substitution rates at 0 mm 2nd event and 0 % external EGR (1600 rpm, 350 Nm), measured values (logarithmic scale)

An increase in external EGR mitigates this behavior and increases the percentage of fully oxidized components, therefore improving the completeness of the combustion. This is shown in Figure 15 through the share of carbon bound in CO_2 emissions for 0 % and 20 % external EGR.

When looking at the peak temperatures during combustion as displayed in Figure 16, the expected reduction in in-cylinder temperature due to external EGR is apparent, which is associated with a drop in nitrogen oxide emissions from 9.83 g/kWh without external EGR to 3.43 g/kWh with an external EGR rate of 20 %.

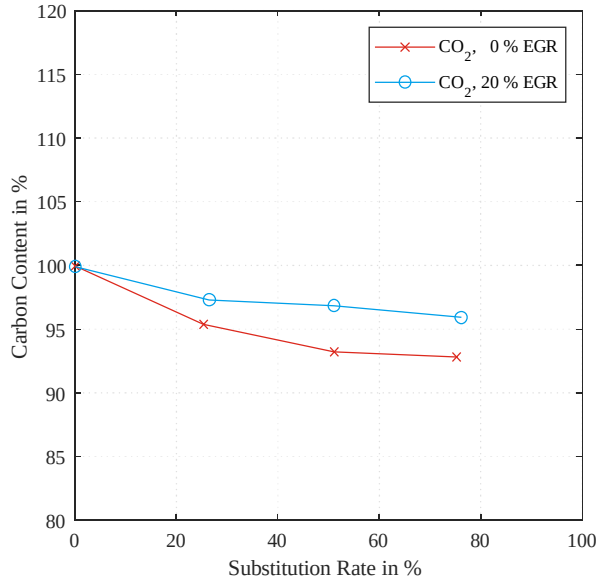

Figure 15. CO_2 share of total carbon emissions at 0 mm 2nd event (1600 rpm, 350 Nm), measured values

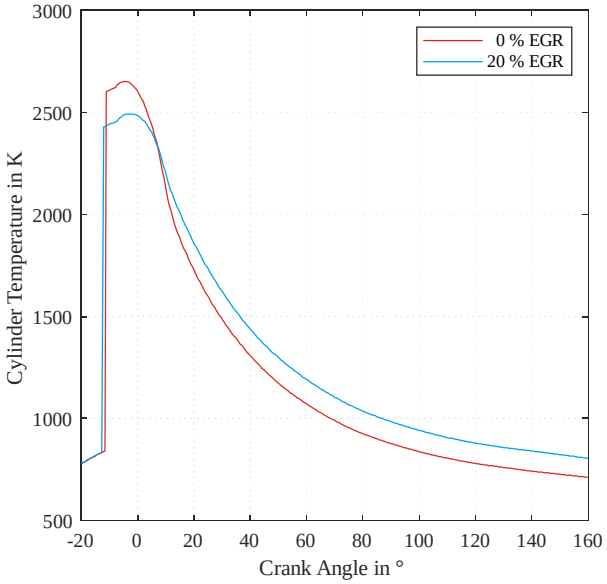

Figure 16. Progression of in-cylinder temperature of the burned zone according to TPA simulation at 0 mm 2nd event and 75 % methane substitution (1600 rpm, 350 Nm), calculated values

The cylinder pressure curves in Figure 17 show a reduction in peak pressure, which supports the results obtained from the TPA calculation. The heat release rates shown in Figure 18 behave similarly for both 0 % and 20 % external EGR.

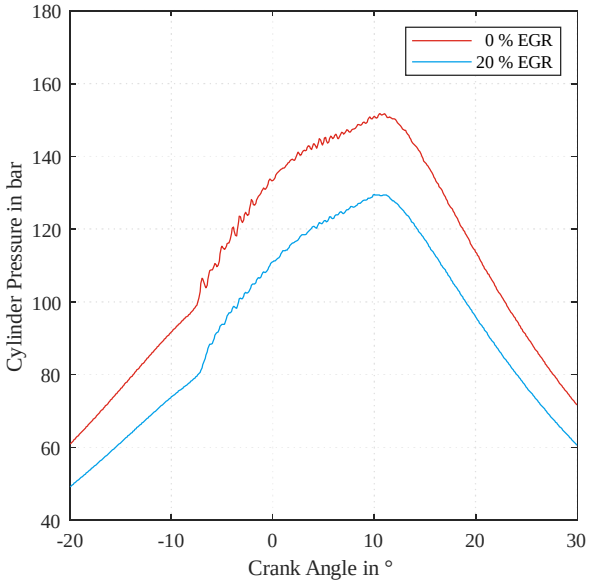

Figure 17. Cylinder pressure curves for 0 and 20 % EGR at 0 mm 2nd event and 75 % methane substitution (1600 rpm, 350 Nm), measured values

For the case of 20 % EGR, a distinct drop of the heat release between the two combustion phases can be seen as the burn duration increases from 18.2 °CA without external EGR to 19.8 °CA. This drop is probably caused by the EGR delaying the ignition of the homogeneous base mixture.
Because of the higher efficiency with external EGR caused by the de-throttling of the engine exhaust, the IMEP of the gas exchange is reduced and therefore less energy needs to be released in the combustion cycle.

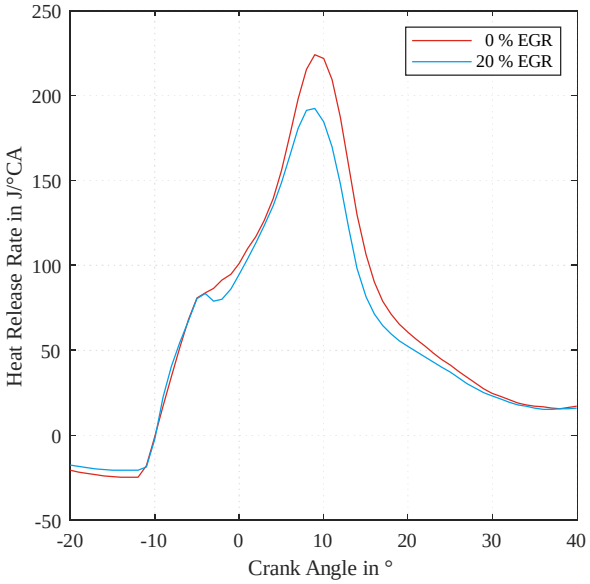

Figure 18. Heat release rates for 0 and 20 % EGR at 0 mm 2nd event and 75 % methane substitution (1600 rpm, 350 Nm), measured values

The reduction of carbon monoxide and methane emissions can be explained by the in-cylinder temperature during the expansion. Figure 16 shows that for an EGR rate of 20 %, the temperature stays at a higher level for a longer period of time compared to the 0 %

EGR case. This means that the temperature is high enough for the oxidation of carbon monoxide and methane for a longer time, elevating the share of the fully oxidized gaseous emissions.

To understand this progression, it is necessary to distinguish between absolute and specific heat capacity of the mixture in the combustion chamber after completion of the gas exchange. Because of its higher temperature, EGR displaces fresh air in the intake manifold. In [18], (chapter “Diesel Engine Combustion”), Binder introduced the terms “replaced EGR” (fresh air in the intake manifold is displaced, i.e. the pressure remains constant with and without EGR) and “additional EGR” (fresh air in the intake manifold remains constant with and without EGR, i.e. the boost pressure needs to be increased). As the test engine used here does not provide any possibility to set the boost pressure, fresh air is displaced by EGR here, and additionally the intake manifold pressure is even reduced. This in turn reduces the mass of gas in the combustion chamber, which lowers the absolute heat capacity of the charge in the cylinder, although the specific heat capacity is higher, see Figure 19.

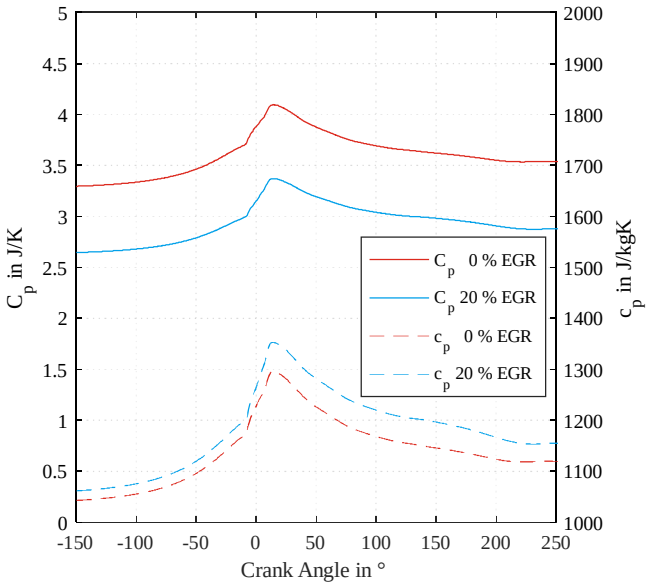

Figure 19. Comparison of absolute and specific heat capacity for 0 and 20 % EGR at 0 mm 2nd event and 75 % methane substitution (1600 rpm, 350 Nm), calculated values

As the heat released by the combustion stays similar due to the engine load point being kept constant, the temperature in the cylinder needs to increase. This also means that the reduction in peak temperatures, and therefore nitrogen oxide emissions, is due to the reduction of the oxygen content as shown in [30] and [31].

By the addition of internal EGR, combustion can be further improved. Using 20 % external EGR rate as a baseline, Figure 20 and Figure 21 show the drop in CO and CH_4 emissions due to the 2nd event valve lift.

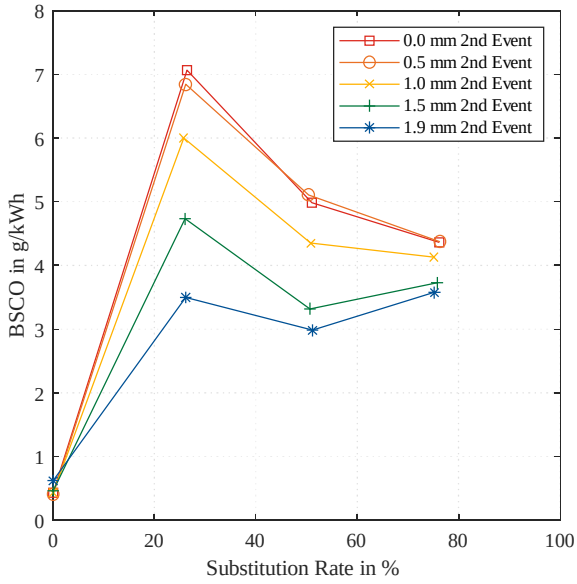

Figure 20. CO emissions depending on substitution rates for different 2nd event valve lifts at 20 % external EGR (1600 rpm, 350 Nm), measured values

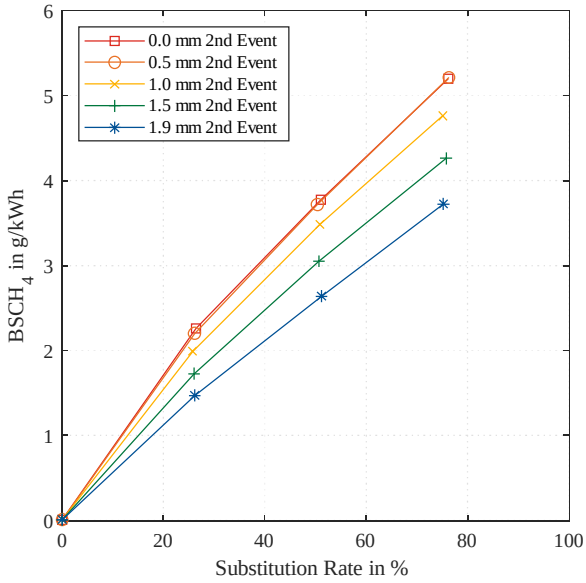

Figure 21. CH_4 emissions depending on substitution rates for different 2nd event valve lifts at 20 % external EGR (1600 rpm, 350 Nm), measured values

The NO_x - soot trade-off for the 2nd event variation is shown in Figure 22. Even though soot emission rises with increasing 2nd event valve lift, it still remains at a very low level. With respect to nitrogen oxides, a slight reduction can be seen with a higher 2nd event lift at the same external EGR rate.

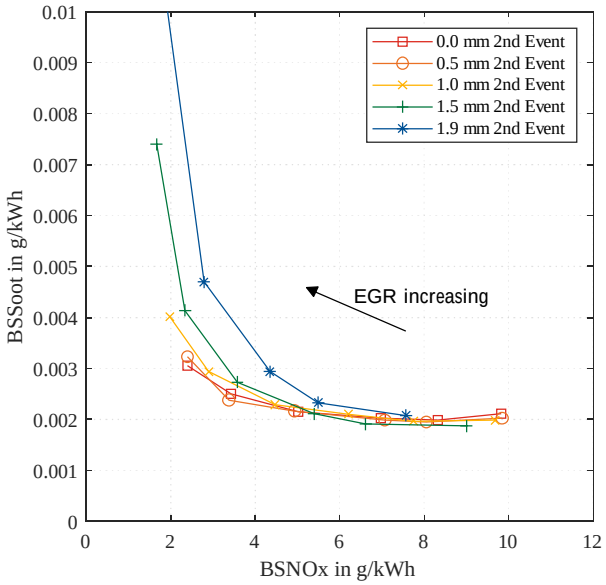

Figure 22. NOx - soot trade-off for different 2nd event valve lifts at a substitution rate of 75 % (1600 rpm, 350 Nm), measured values

To put these 2nd event valve lifts in relation to the external EGR rate, it is necessary to calculate the residual gas fraction after completion of gas exchange by means of TPA. Figure 23 shows the results of this calculation.

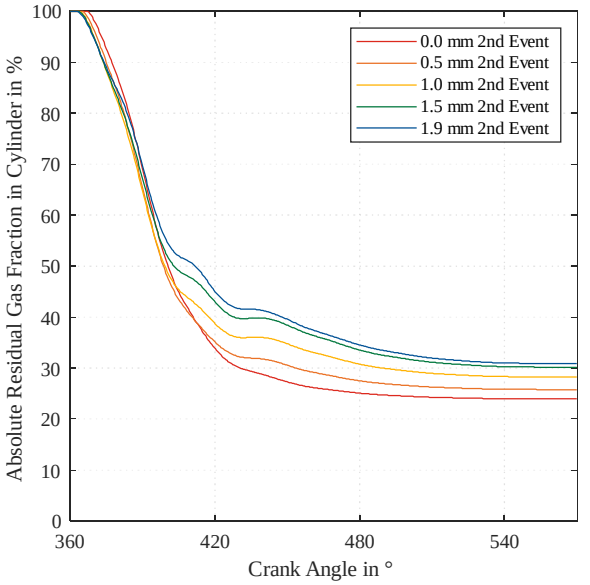

Figure 23. Residual gas fractions in combustion chamber during gas exchange for different 2nd event valve lifts and 20 % external EGR (1600 rpm, 350 Nm), calculated values

Although the fraction of residual gas inside the combustion chamber is increased and the maximum cylinder pressure is decreased (see Figure 24), the burn duration remains constant, as can be seen from Figure 25.

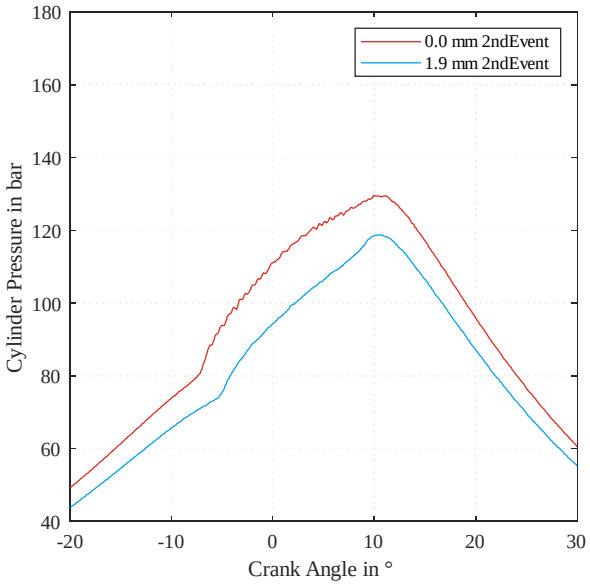

Figure 24. Cylinder pressure curves for 0 and 1.9 mm 2nd event at 20 % external EGR and 75 % methane substitution (1600 rpm, 350 Nm), measured values

Even though the diesel injection takes place 2 °CA later with 1.9 mm 2nd event, the center of combustion is situated at 8 °CA ATDC for both cases. The reduced drop in heat release between the two phases of combustion and the more rapid heat release in the second phase are the reason for this behavior. As the combustion is more complete and the gas exchange losses decrease with increasing 2nd event, the engine efficiency increases, which in return leads to a reduction in energy input through the two fuels.

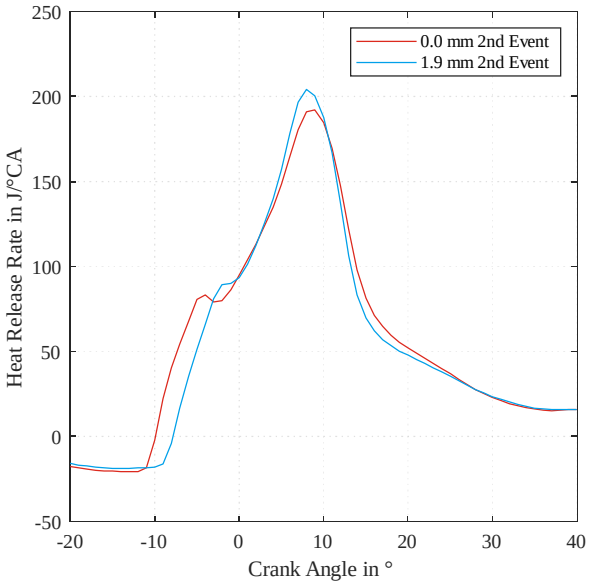

Figure 25. Heat release rates for 0 and 1.9 mm 2nd event at 20 % external EGR and 75 % methane substitution (1600 rpm, 350 Nm), measured values

6. Summary and Conclusions

In the presented work, the effects of different types of exhaust gas recirculation (EGR) on a nonroad diesel-methane dual-fuel engine were investigated for several substitution rates. The focus was on nitrogen oxide, soot, carbon monoxide and methane emissions. First, the amount of EGR was set by a cooled, external exhaust gas recirculation system. Then, internal EGR was added by a second exhaust valve lift ("2nd event").

Increasing substitution rates in diesel-methane dual-fuel combustion mitigate the trade-off of nitrogen oxides vs. soot. This makes it possible to use higher EGR rates, which are necessary to reduce the carbon monoxide and methane emissions caused by the homogeneous combustion of methane.

The presented experiments show that external EGR is already a very effective measure to reduce nitrogen oxide, carbon monoxide and methane emissions. However, adding internal EGR by a second exhaust valve lift helps to reduce these emissions even further, which underlines the particular usefulness of this measure for dual-fuel engines. As all values continued to improve when approaching the maximum possible 2nd event valve lift, it is assumed that even more internal EGR would be beneficial. This will be the subject of future investigations with a modified setup for increased internal EGR.

As it is not possible to completely eliminate these pollutant components in the exhaust by the introduction of EGR into the combustion process, an exhaust aftertreatment system will still be necessary. Therefore, investigations to raise the exhaust gas temperature in order to ensure sufficient conversion in the catalytic converter also need to be carried out. [32] shows examples of such measures, which could partly also be applied to a dual-fuel engine.

References

[1] Chaichan, M. T. "Combustion of Dual Fuel Type Natural Gas/Liquid Diesel Fuel in Compression Ignition Engine." 2014. *IOSR Journal of Mechanical and Civil Engineering*, no. 6: 48–58. https://doi.org/10.9790/1684-11644858.

[2] Pettinen, R., Kaario, O., and Larmi, M. "Dual-Fuel Combustion Characterization on Lean Conditions and High Loads." 2017. *SAE Technical Paper 2017-01-0759*. https://doi.org/10.4271/2017-01-0759.

[3] Benajes, J., Garcia, A., Monsalve-Serrano, J., and Boronat, V. "Dual-Fuel Combustion for Future Clean and Efficient Compression Ignition Engines." 2017. *Applied Sciences*. https://doi.org/10.3390/app7010036.

[4] Hall, E. "Dual Fuel Medium Speed Engines for Transportation." 2014. *AVL large engine tech days 2014*.

[5] Yu, C., Wang, J., Wang, Z., and Shuai, S. "Comparative study on Gasoline Homogeneous Charge Induced Ignition (HCII) by diesel and Gasoline/Diesel Blend Fuels (GDBF) combustion." 2013. *Fuel* 106:470–77. https://doi.org/10.1016/j.fuel.2012.10.068.

[6] Stanglmaier, R. H., Ryan, T. W., and Souder, J. S. "HCCI Operation of a Dual-Fuel Natural Gas Engine for Improved Fuel Efficiency and Ultra-Low NOx Emissions at Low to Moderate Engine Loads." 2001. *SAE Technical Paper 2001-01-1897*. https://doi.org/10.4271/2001-01-1897.

[7] Kokjohn, S. L., Hanson, Reed M., Splitter, D. A., and Reitz, R. D. "Experiments and Modeling of Dual-Fuel HCCI and PCCI Combustion Using In-Cylinder Fuel Blending." 2009. *SAE Int. J. Engines* 2 (2): 24–39. https://doi.org/10.4271/2009-01-2647.

[8] Reitz, R. D., and Duraisamy, G. "Review of high efficiency and clean reactivity controlled compression ignition (RCCI) combustion in internal combustion engines." 2015. *Progress in Energy and Combustion Science*, 12–71. https://doi.org/10.1016/j.pecs.2014.05.003.

[9] Kokjohn, S. L., Hanson, R. M., Splitter, D. A., and Reitz, R. D. "Fuel reactivity controlled compression ignition (RCCI): a pathway to controlled high-efficiency clean combustion." 2011. *International Journal of Engine Research*, 209–26. https://doi.org/10.1177/1468087411401548.

[10] Eise, F., Heinz, L., Wagner, U., and Koch, T. "RCCI in Heavy Duty Engines." *THIESEL 2020 Conference on Thermo- and Fluid Dynamic Processes in Direct Injection Engines*.

[11] Paykani, Amin, Kakaee, Amir-Hasan, Rahnama, Pourya, and Reitz, Rolf D. "Progress and recent trends in reactivity-controlled compression ignition engines." 2016. *International Journal of Engine Research* 17 (5): 481–524. https://doi.org/10.1177/1468087415593013.

[12] U.S. Department of Energy "Renewable Natural Gas Production." https://afdc.energy.gov/fuels/natural_gas_renewable.html.

[13] Sterner, M. "Bioenergy and renewable power methane in integrated 100% renewable energy systems." 2009. Ph.D. thesis, Kassel University Press GmbH.

[14] Robinson, C., and Smith, D. B. "The Auto-Ignition Temperature of Methane." 1984. *Journal of Hazardous Materials*, 199–203.

[15] Lehtoranta, K., Koponen, P., Vesala, H., Kallinen, K., and Maunula, T. "Performance and Regeneration of Methane Oxidation Catalyst for LNG Ships." 2021. *Journal of Marine Science and Engineering*, 111. https://doi.org/10.3390/jmse9020111.

[16] Umweltbundesamt "Global Warming Potential (GWP) of certain substances and mixtures." https://www.umweltbundesamt.de/en/document/global-warming-potential-gwp-of-certain-substances.

[17] Sjoeberg, M., Dec, J., and Hwang, W. "Thermodynamic and Chemical Effects of EGR and Its Constituents on HCCI Autoignition." 2007. *SAE Technical Paper 2007-01-0207*. https://doi.org/10.4271/2007-01-0207.

[18] Mollenhauer, K., and Tschoeke, H. *Handbook of Diesel Engines*. 2010: Springer-Verlag Berlin Heidelberg.

[19] Dev, S., Guo, H., Lafrance, S., and Liko, B. "An Experimental Study on the Effect of Exhaust Gas Recirculation on a Natural Gas-Diesel Dual-Fuel Engine." 2020. *SAE Technical Paper 2020-01-0310*. https://doi.org/10.4271/2020-01-0310.

[20] Shim, E. J., Park, H., and Bae, C. "Effects of Hot and Cooled EGR for HC Reduction in a Dual-Fuel Premixed Charge Compression Ignition Engine." 2018. *SAE Technical Paper 2018-01-1730*. https://doi.org/10.4271/2018-01-1730.

[21] Buitkamp, T. "Potenziale eines Dieselmotors mit variablem Ventiltrieb und Zylinderzuschaltung in einem Traktor." [Potentials of a Diesel Engine with a Variable Valve Train and

Cylinder Activation in a Tractor]. 2019. Ph.D. Thesis, Technische Universitaet Berlin.

[22] Thees, M., Buitkamp, T., Guenthner, M., and Pickel, P. “High efficiency diesel engine concept with variable valve train and cylinder deactivation for integration into a tractor.” In *ASME 2019 Internal Combustion Engine*.

[23] Gonzalez D., Manuel A., and Di Nunno, D. “Internal Exhaust Gas Recirculation for Efficiency and Emissions in a 4-Cylinder Diesel Engine.” 2016. *SAE Technical Paper 2016-01-2184*. https://doi.org/10.4271/2016-01-2184.

[24] Willand, J., Jelitto, C., and Jakobs, J. “The GCI combustion process from Volkswagen.” 2008. *MTZ Worldw* 69 (4): 56–61. https://doi.org/10.1007/BF03226906.

[25] European Parliament and Council “Regulation (EU) 2016/1628 of the European Parliament and of the Council.” 2016. https://eur-lex.europa.eu/legal-content/DE/ALL/?uri=CELEX%3A32016R1628.

[26] Buitkamp, T., Guenthner, M., Mueller, F., and Beutler, T. “A Detailed Study of a Cylinder Activation Concept by Efficiency Loss Analysis and 1D Simulation.” 2020. *Automotive and Engine Technology Volume 5*, 159–72. https://doi.org/10.1007/s41104-020-00070-1.

[27] Plee, S. L., Ahmad, T., and Myers, J. P. “Flame Temperature Correlation for the Effects of Exhaust Gas Recirculation on Diesel Particulate and NOx Emissions.” 1981. *SAE Technical Paper 811195*. https://doi.org/10.4271/811195.

[28] Heywood, J. B. *Internal Combustion Engine Fundamentals*. 2018: McGraw-Hill Education.

[29] Magno, A., Mancaruso, E., and Vaglieco, B. “Combustion Analysis of Dual Fuel Operation in Single Cylinder Research Engine Fuelled with Methane and Diesel.” 2015. *SAE Technical Paper 2015-24-2461*. https://doi.org/10.4271/2015-24-2461.

[30] Plee, S. L., Ahmad, T., Myers, J. P., and Faeth, G. M. “Diesel NOx Emissions - A Simple Correlation Technique for Intake Air Effects.” 1982. *Nineteenth Symposium (International) on Combustion*. https://doi.org/10.1016/S0082-0784(82)80326-3.

[31] Ahmad, T., and Plee, S. L. “Application of Flame Temperature Correlations to Emissions from a Direct-Injection Diesel Engine.” 1983. *SAE Technical Paper 831734*. https://doi.org/10.4271/831734.

[32] Thees, M., Guenthner, M., and Mueller, F. “Thermal Management Concept for the Exhaust Aftertreatment of Commercial Vehicle Diesel Engines Using Variable Mixtures of Diesel Fuel and Rapeseed Oil.” 2021. *SAE Technical Paper 2021-01-0498*. https://doi.org/10.4271/2021-01-0498.

Contact Information

Dipl.-Ing. Florian Mueller

University of Kaiserslautern (TUK), Germany
Institute of Vehicle Propulsion Systems (LAF)
D-67663 Kaiserslautern/Germany

E-Mail: florian.mueller@mv.uni-kl.de

Acknowledgments

The work presented here was carried out within the framework of the project "HKMVK", funded by the German Federal Ministry of Food and Agriculture (BMEL) with the Agency for Renewable Resources (FNR) as project management organization. The authors would like to express their gratitude for this funding.
Furthermore, the authors would like to thank the associated project partner John Deere for their support throughout the project.

Definitions / Abbreviations

°CA	degree crank angle
ATDC	after top dead center
BtG	biomass to gas
BDC	bottom dead center
BMEP	brake mean effective pressure
BSCO	break specific carbon monoxide emissions
BSNOx	break specific nitrogen oxides emissions
$BSCH_4$	break specific methane emissions
c_p	specific heat capacity
C_p	absolute heat capacity
CH_4	methane
CNG	compressed natural gas
CO	carbon monoxide
CO_2	carbon dioxide
DOHC	double overhead camshaft
EGR	exhaust gar recirculation
EV	exhaust valve
GWP	global warming potential
HC	hydrocarbons
H_2O	water
IMEP	indicated mean effective pressure

IV	intake valve
λ	lambda: air to fuel ratio
LHV	lower heating value
LTC	low temperature combustion
$\dot{m}$	mass flow
MPa	megapascal
NO	nitrogen oxide
NO_2	nitrogen dioxide
NO_x	nitrogen oxides (NO + NO_2)
NRSC	non-road steady cycle
OHV	overhead valves
PM	particulate mass
PN	particulate number
PtG	power to gas
RCCI	reactivity controlled compression ignition
rpm	revolutions per minute
SOI	start of injection
TDC	top dead center
TPA	three pressure analysis
WHSC	world harmonized stationary cycle